EUR REV MED PHARMACOL SCI
2026; 30: 113-125

TISSUE-SPECIFIC ADAPTIVE RESPONSES OF THE VITAMIN D_3 AUTO-/PARACRINE SYSTEM TO VITAMIN D_3 DEFICIENCY IN BONE AND BRAIN

I. SHYMANSKYI[1], O. LISAKOVSKA[1], A. KHOMENKO[1], V. BILOUS[2], Y. KUCHERIAVYI[3], I. POLADYCH[4], Y. PARKHOMENKO[1], M. VELIKY[1]

[1]Department of Biochemistry of Vitamins and Coenzymes, Palladin Institute of Biochemistry, National Academy of Sciences of Ukraine, Kyiv, Ukraine
[2]Department of Enzyme Chemistry and Biochemistry, Palladin Institute of Biochemistry, National Academy of Sciences of Ukraine, Kyiv, Ukraine
[3]Department of Protein Structure and Function, Palladin Institute of Biochemistry, National Academy of Sciences of Ukraine, Kyiv, Ukraine
[4]Department of Obstetrics and Gynecology No 1, Bogomolets National Medical University, Kyiv, Ukraine

Corresponding Author
Ihor Shymanskyi, Ph.D; e-mail: ihorshym@gmail.com

ABSTRACT – *Objective:* We hypothesized that vitamin D_3 (VD_3) coordinates a complex functional interplay between cerebral homeostasis and skeletal integrity by modulating mineral metabolism and osteotropic signaling. This neuroskeletal axis is likely mediated *via* a feedback loop involving fibroblast growth factor 23 (FGF23), a key regulator within both osseous and cerebral tissues. In this context, our study aimed to characterize tissue-specific adaptive responses by analyzing correlations between components of the vitamin D_3 system and FGF23 signaling under physiological and VD_3-deficient conditions.

Materials and Methods: Twenty-four female Wistar rats were randomized into three experimental groups: intact (standard diet), VD_3-deficient (vitamin-free diet), and repletion. The latter underwent an initial two-month depletion phase followed by one month of therapeutic VD_3 supplementation (1,000 IU/kg b.w.). Serum 25(OH)D_3, PTH, and FGF23 levels (circulating and tissue-specific) were quantified *via* ELISA. The expression of the vitamin D_3 receptor (VDR), vitamin D_3-binding protein (VDBP), and hydroxylases CYP27B1 and CYP24A1 in cerebral and osseous lysates was determined *via* Western blotting.

Results: Dietary VD_3 deficiency triggered systemic metabolic disturbances, including reduced serum 25(OH)D_3, hypocalcemia, secondary hyperparathyroidism, and elevated systemic FGF23. Tissue analysis revealed shared compensatory responses in both compartments, notably the induction of VDBP and CYP27B1. However, osseous regulation appeared to be dominated by systemic feedback loops (the FGF23/CYP24A1 correlation), whereas the brain exhibited distinct regulatory patterns, characterized by reduced VDR and CYP24A1 despite stable local FGF23 levels. Following VD_3 replenishment, systemic and bone markers normalized, yet cerebral VDR levels remained persistently low.

Conclusions: VD_3 deficiency triggers divergent, tissue-specific regulatory responses, suggesting that the brain may preserve a more stable internal environment than osseous tissue. These findings reflect a degree of cerebral metabolic regulation distinct from the systemic endocrine susceptibility driven by the FGF23 axis. However, the functional significance of these localized patterns and their underlying neuroprotective implications requires further comprehensive and robust experimental validation.

KEYWORDS: Brain-bone axis, FGF23, VDR, CYP27B1, CYP24A1, Vitamin D_3-binding protein, Mineral metabolism, Neuroprotection, Osteotropic proteins, Cholecalciferol.

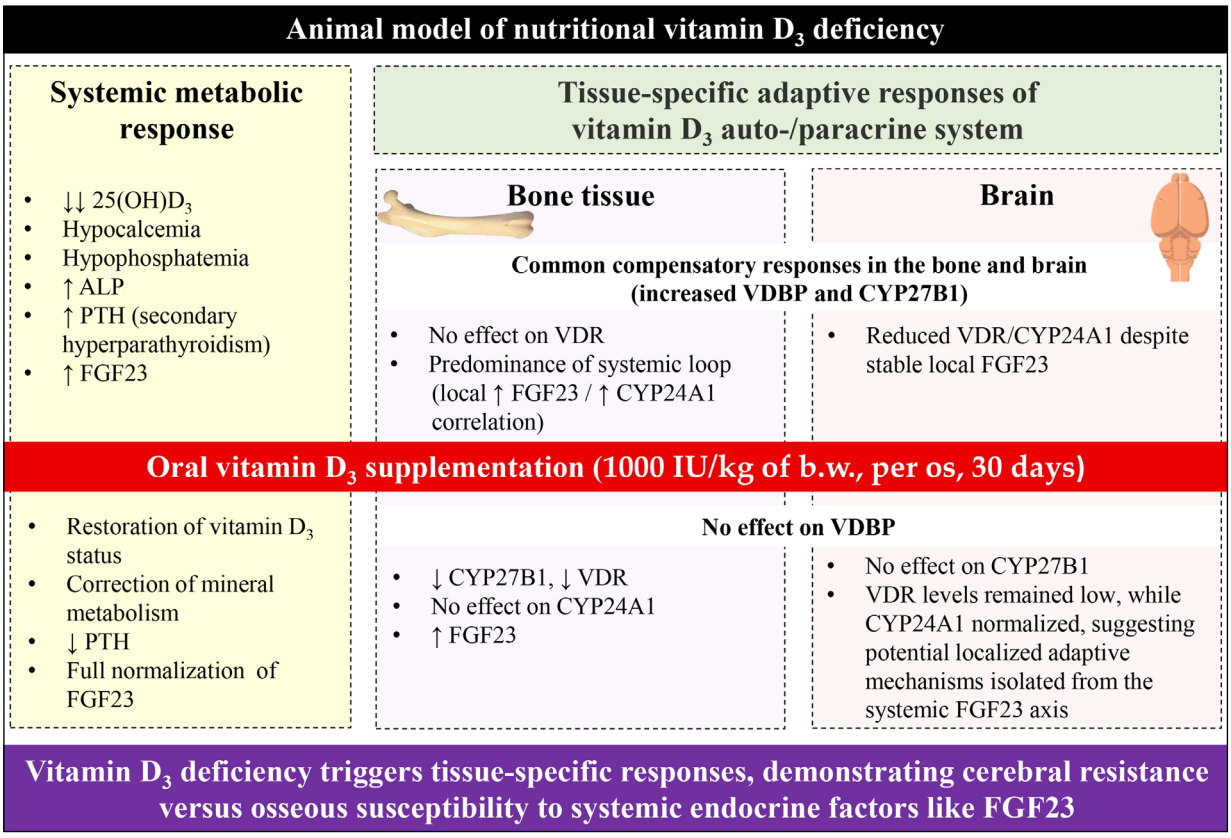

Graphical Abstract. Schematic representation of tissue-specific responses to vitamin D_3 (VD_3) deficiency and oral supplementation (1,000 IU/kg). VD_3 deficiency induces systemic alterations (hypocalcemia, ↑PTH, ↑FGF23). Bone responses follow systemic endocrine regulation (FGF23–CYP24A1 axis), whereas the brain shows distinct local adaptations, including reduced VDR despite stable FGF23. Supplementation restores systemic and osseous parameters but not cerebral VDR, indicating tissue-specific regulation.

INTRODUCTION

Vitamin D_3 (cholecalciferol, VD_3) deficiency is a widespread health concern associated with disruptions in calcium-phosphate metabolism, immune function, and neurological integrity[1]. It is estimated that around 80% of the global adult population experiences mild to moderate vitamin D_3 hypovitaminosis. Clinically, this deficiency manifests as rickets in children and as osteoporosis, osteomalacia, muscle weakness, or immunodeficiency in adults. Furthermore, chronic VD_3 deprivation correlates strongly with increased risks of autoimmune diseases, vascular disorders, reproductive dysfunction, and potential cognitive impairment[1,2].

Cholecalciferol is the most biologically vital form for humans. Primarily synthesized in the skin (80%) *via* UV irradiation of 7-dehydrocholesterol and supplemented by dietary intake (20%), both endogenous and exogenous forms are initially inert[3]. Activation requires a two-stage hydroxylation process: first, hepatic conversion to 25-hydroxyvitamin D_3 (calcidiol, $25(OH)D_3$), the standard diagnostic biomarker of VD_3 status; and second, the predominantly renal conversion by 1α-hydroxylase to the hormonally active 1α,25-dihydroxyvitamin D_3 (calcitriol, $1\alpha,25(OH)_2D_3$). Calcitriol exerts its pleiotropic effects *via* the ubiquitous vitamin D_3 receptor (VDR)[3,4]. The production of this active hormone is under tight feedback regulation involving parathyroid hormone (PTH) and fibroblast growth factor 23 (FGF23)[5,6]. FGF23, secreted by osteocytes and osteoblasts, acts as a major phosphaturic hormone (phosphatonin) that promotes renal phosphate excretion and suppresses intestinal phosphate absorption. Critically, FGF23 modulates VD_3 metabolism by directly inhibiting renal CYP27B1 (1α-hydroxylase), while stimulating CYP24A1 (24-hydroxylase), which facilitates calcitriol degradation[6,7]. Thus, FGF23 serves as a fundamental endocrine link coordinating phosphorus homeostasis with the systemic regulation of VD_3 activity.

Recent recognition of the nervous system's contribution to bone remodeling has driven extensive research into the neuro-osseous interplay, often referred to as the brain-skeleton axis. Compelling clinical evidence indicates that neurological diseases often involve altered osseous physiology, leading to reduced bone mineral density and strength, which ultimately manifests as osteopenia and osteoporosis[8]. This neuroskeletal

axis encompasses complex metabolic, sensory, and endocrine interconnections. Both the sympathetic and parasympathetic nervous systems influence skeletal health through diverse signaling pathways involving mediators such as leptin, serotonin, dopamine, glutamate, adiponectin, and neuropeptide Y[9,10]. Conversely, the relationship between the nervous system and skeletal tissue appears reciprocal. Bone-derived proteins, including osteocalcin, osteopontin, and sclerostin, have demonstrated significant *in vivo* effects on the central nervous system (CNS)[11]. Notably, the osteogenic hormone osteocalcin is essential for activating the acute stress response by inhibiting parasympathetic signaling[12]. It crosses the blood-brain barrier to enhance the synthesis of serotonin, dopamine, and norepinephrine, while modulating γ-aminobutyric acid (GABA) secretion through binding to the orphan receptor GPR158 in brainstem, midbrain, and hippocampal neurons[13]. This endocrine crosstalk underscores a bidirectional link between psychological stress and bone health; specifically, the development of osteoporosis is linked to hypothalamic-pituitary-adrenal axis activation. This pathway – driven by glucocorticoids and altered growth factor responses, such as insulin-like growth factor 1 (IGF-1) – collectively impairs osseous mass preservation[14].

While the roles of osteocalcin and IGF-1 in this bidirectional axis are becoming clear, emerging evidence suggests that FGF23 – traditionally viewed as a renal-osseous regulator – also functions within the CNS through its co-receptor, Klotho[15]. Beyond its well-established role in VD_3 and mineral metabolism, adequate levels of FGF23 appear integral for normal neurological functions. Specifically, pathologically high circulating FGF23 levels, frequently observed in chronic kidney disease, are associated with cognitive impairment, reduced hippocampal ATP, increased stroke risk, and structural defects in the cerebral white matter, potentially mediated by vascular damage or direct neuronal toxicity[15-17]. In contrast, a previous study in mice showed that a complete loss of FGF23 function leads to severe neurodevelopmental abnormalities independently of Klotho expression, revealing a direct role for FGF23 signaling in the brain[18]. However, it remains unclear whether these effects are purely systemic or involve localized cerebral FGF23 homeostatic mechanisms.

Our hypothesis centers on the capacity of VD_3 to act as a key coordinator of the functional crosstalk between cerebral homeostasis and skeletal status by fine-tuning mineral metabolism and osteoendocrine signaling pathways. This neuroskeletal network is likely maintained by the established role of VD_3 in maintaining mineral balance and the regulation of bone-derived protein synthesis. We propose that variations in VD_3 status modulate the expression of VD_3-metabolizing enzymes and VDR-mediated signaling across both osseous and cerebral tissues. This axis is integrated with FGF23, which functions within a reciprocal regulatory feedback loop with VD_3 and PTH. Given that FGF23 is expressed in the brain, it may serve as an under-explored component of the neuro-osseous interaction. This study investigates the tissue-specific expression profiles of VD_3 auto-/paracrine system components (VDR, VDBP, CYP27B1, CYP24A1) and FGF23 levels in bone and brain tissues, and evaluates their correlation with systemic VD_3 status under both physiological and experimentally induced VD_3-hypovitaminosis conditions.

MATERIALS AND METHODS

Animals and experimental design

This study was carried out using female Wistar rats (State Enterprise "L.I. Medved's Research Center of Preventive Toxicology, Food and Chemical Safety" of the Ministry of Health of Ukraine, Kyiv, Ukraine; 5-6 weeks old upon arrival; n = 24) housed in a temperature-controlled room (21 ± 2°C). While the facility maintained a standard 12-h light-dark cycle, the light phase was specifically adjusted for the experimental groups to limit endogenous vitamin D_3 synthesis. All rats were fed a standard laboratory diet and had *ad libitum* access to tap water. After a 1-week acclimatization period, the female rats weighing 132.33±6.99 g were randomly divided into three groups (n=8 for each group) and maintained for three months: 1) the intact group (VD_3 sufficiency), 2) the VD_3-deficient group, and 3) the VD_3-supplemented group, which received cholecalciferol (1,000 IU/kg of body weight, *per os*) for 1 month following a two-month VD_3-depletion period.

In contrast to the intact animals, which consumed a normal, balanced growth diet (REZON-1, Ukraine), the rodents in the deficient and supplemented groups were fed a custom-prepared, normocalcemic, VD_3-deficient diet. The nutrient composition of this diet included 60% carbohydrates, 18% protein, and 7% fat, along with water-soluble and fat-soluble vitamins (excluding VD_3). Micronutrients consisted of 5.2 g/kg calcium carbonate and 2.8 g/kg inorganic phosphate salt. To prevent endogenous vitamin D_3 synthesis, the VD_3-deficient and supplemented (during the depletion phase) animals were also kept in partial darkness by limiting their light exposure to six hours per day. Body weights were recorded weekly throughout the study. Finally, all rats were anesthetized (1.9% diethyl ether) and humanely decapitated. The brain and femora were quickly dissected and

transferred to specialized buffers according to the downstream procedures. All samples that were not used immediately were stored at -80°C.

Given the significantly higher prevalence of osteoporosis in human females compared to males, this study focused exclusively on the female Wistar rat model to investigate the skeletal and cerebral response to vitamin D_3 dynamics. We utilized young female rats (5-6 weeks old), a critical life stage coinciding with peak active skeletal growth and the onset of puberty, to robustly model the long-term impact of vitamin D_3 deficiency during developmental periods. The use of a single-sex, genetically uniform outbred cohort facilitated reliable data analysis by minimizing individual physiological variance and eliminating confounding variables arising from sex-based hormonal differences.

Animal handling and experimental protocols complied with international bioethical principles and ARRIVE (Animal Research: Reporting of *In Vivo* Experiments) guidelines. The study was approved by the Animal Care Ethics Committee of the Palladin Institute of Biochemistry (Protocol #3, February 26, 2024).

Biochemical analysis of serum

Blood samples were collected *via* cardiac puncture under anesthesia. Serum PTH and FGF23 concentrations were determined using the Rat PTH ELISA kit (RTFI00259; Assay Genie, Ireland) and the Rat FGF23 ELISA kit (RTFI00086; Assay Genie, Ireland), respectively. Total 25(OH)D_3 levels were measured using the Rat Vitamin D total ELISA kit (DE1971; Demeditec Diagnostics GmbH, Germany). Serum mineral components (calcium and inorganic phosphate) were quantified using commercially available assay kits (ab102505 and ab65622, respectively; Abcam, UK). All assays were performed in strict accordance with the manufacturers' protocols.

Total alkaline phosphatase (ALP) activity in blood serum was determined by measuring the formation of 4-nitrophenol resulting from the enzymatic cleavage of 4-nitrophenylphosphate[19]. The reaction was terminated by adding a 30 mM solution of EDTA (Trilon B) in 1M NaOH. The optical density of the samples was measured spectrophotometrically at λ = 410 nm. To distinguish between ALP isoenzymes, a differential inactivation approach was employed. The activity of the bone-specific ALP isoform was calculated as the difference between total ALP activity and the heat-stable ALP fraction, determined after incubating samples in a water bath at +56-57°C to inactivate heat-labile isoforms. Additionally, the activity of the intestinal ALP isoenzyme was assessed using 5 mM L-phenylalanine as a specific inhibitor.

Preparation of tissue homogenates for FGF23 analysis

Homogenization was performed using standardized protocols adapted to the specific morphological characteristics of each biological matrix. Specimens from the whole brain and femurs were initially snap-frozen in liquid nitrogen and subsequently mechanically pulverized into a fine powder using a pre-cooled mortar and pestle to maximize the surface area for protein recovery. To ensure maximum stability, all subsequent extraction and demineralization steps were conducted at 4°C in buffers supplemented with a broad-spectrum protease inhibitor cocktail (1% v/v; P8340, Sigma-Aldrich, St. Louis, MO, USA), containing AEBSF, aprotinin, bestatin, E-64, leupeptin, and pepstatin A.

While the pulverized cerebral specimens were stored at -80°C to prevent degradation, osseous samples underwent a specialized demineralization step in a 14% EDTA solution (pH 7.4; prepared in ultrapure water and adjusted with NaOH) at a 1:20 (w/v) ratio for 10-14 days under constant gentle agitation. This procedure was designed to facilitate the complete recovery of matrix-bound proteins from the mineralized bone phase. After demineralization was complete, the powder specimens were weighed and homogenized in ice-cold phosphate-buffered saline (PBS) at a 1:10 (w/v) ratio.

Subsequently, both the cerebral homogenates and the demineralized bone suspensions were subjected to ultrasonication on ice (3 cycles of 10 s at 20 kHz) to ensure efficient cell lysis and the release of all intracellular and matrix-associated proteins. Homogenates were then centrifuged (5,000 × g, 10 min, 4°C) to remove cellular and mineral debris. Total protein concentrations in the resulting supernatants were determined by the Lowry method and standardized to 5 mg/mL to ensure analytical consistency across all samples.

Quantification and validation of tissue FGF23

Tissue FGF23 levels were quantified using the Rat FGF23 ELISA kit (RTFI00086; Assay Genie, Ireland). To address potential matrix effects in tissue homogenates, the validity of this experimental procedure was confirmed *via* linearity-of-dilution tests. High-concentration cerebral and osseous samples were serially diluted (1:2, 1:4, 1:8, and 1:16) using the standardized sample diluent. These evaluations demonstrated a strong linear recovery (R^2 > 0.98) within the assay's dynamic range (15.625-1,000 pg/mL), indicating that the tissue matrices did not significantly interfere with antibody–antigen interaction.

For the experimental analysis, standardized supernatants (5 mg/mL total protein) were used to ensure that FGF23 concentrations remained within the detection limit. Raw values were normalized to each sample's total protein content, and final tissue FGF23 levels were expressed as picograms per milligram of total protein (pg/mg protein). This normalization approach accounts for potential variations in tissue density and extraction efficiency, enabling a reliable comparison across experimental groups.

Western blotting

Protein lysates were obtained from brain and bone samples by treatment with RIPA lysis buffer [50 mM Tris-HCl (pH 7.4), 150 mM NaCl, 1 mM EDTA, 1% Triton X-100, 1% sodium deoxycholate, and 0.1% SDS] supplemented with the same broad-spectrum protease inhibitor cocktail (1% v/v; Sigma-Aldrich, St. Louis, MO, USA) used for the FGF23 analysis. Notably, while osseous samples for FGF23 quantification required prolonged demineralization, proteins for Western blotting were extracted directly from the pulverized bone powder using RIPA buffer to preserve the integrity of the target markers. Samples were subsequently subjected to sonication on ice to achieve complete cell lysis. To standardize quantification across the distinct cerebral and osseous matrices, a two-tier normalization strategy was employed. Total protein concentration was initially determined by the Lowry method, and all samples were adjusted to a uniform loading of 40 µg per lane.

Protein lysates were heated in a sample buffer containing β-mercaptoethanol (Sigma-Aldrich, St. Louis, MO, USA) (95°C, 5 min) and separated *via* 10% Tris-Glycine SDS-PAGE[20]. Molecular weights were confirmed using the Spectra Multicolor Broad Range Prestained Protein Ladder (#26634, Thermo Fisher Scientific, Waltham, MA, USA). Following electrophoresis, proteins were transferred to nitrocellulose membranes, which were blocked with 5% non-fat milk and incubated overnight at 4°C with primary antibodies against VDBP (1:1000, NBP1-88027, Novus Biologicals, Centennial, CO, USA), VDR (1:500, NBP2-66778, Novus Biologicals, Centennial, CO, USA), CYP27B1 (1:500, PA5-26065, Thermo Fisher Scientific, Waltham, MA, USA), CYP24A1 (1:500, PA5-79127, Thermo Fisher Scientific, Waltham, MA, USA), or β-actin (1:10,000, A3854, Sigma-Aldrich, St. Louis, MO, USA). Protein signals were detected using an anti-rabbit horseradish peroxidase-conjugated secondary antibody (1:1000, #1706515, Bio-Rad, Hercules, CA, USA) and developed with the following chemiluminescent agents: p-coumaric acid (C9008, Sigma-Aldrich, St. Louis, MO, USA) and luminol (A4685, AppliChem GmbH, Darmstadt, Germany).

To ensure precise normalization, target proteins were analyzed on parallel gels loaded with identical samples from a single master mix. In this approach, β-actin served as a common internal loading control, confirming equal protein loading across all gels in each experimental run. Densitometric quantification was performed using the Gel-Pro Analyzer v3.1 software, in which the signal intensity of each target protein was normalized to its corresponding β-actin signal from the parallel run. For CYP27B1 and CYP24A1, although secondary minor bands were occasionally observed (likely representing tissue-specific isoforms or post-translational modifications), only the specific bands aligning with the validated molecular weights (~56 kDa and ~59 kDa, respectively) were included in the analysis. Notably, comparisons of protein expression were conducted strictly within each specific tissue type (brain or bone) across experimental groups. This approach precluded absolute quantitative comparisons between cerebral and osseous tissues, due to inherent differences in tissue density and extraction efficiency.

Statistical analysis

Statistical analysis was performed using Origin Pro 8.5 software (OriginLab Corporation, Northampton, MA, USA). The normality of data distribution was verified using the Shapiro-Wilk test. Data are presented as mean ± standard deviation (SD). Comparisons between two groups were performed using the Student's *t*-test, while multiple group evaluations were conducted using one-way analysis of variance (ANOVA) followed by Tukey's *post-hoc* test. A value of $p < 0.05$ was considered statistically significant. All analyses were based on the number of individual animals per group ($n = 8$).

RESULTS

Biochemical analyses (Table I) demonstrate that dietary VD_3 deprivation in the deficient group led to a substantial reduction – exceeding 6-fold – in circulating $25(OH)D_3$ content. As this stable, predominant cholecalciferol metabolite reliably reflects systemic vitamin VD_3 status and bioavailability, its diminished concentration validates the success of the experimental model. Furthermore, this condition resulted in a 1.6-fold increase in total alkaline phosphatase activity in serum compared with the intact group. This enzyme facilitates the hydrolysis of phosphoric acid mon-

Table I. Serum mineral components, PTH, FGF23, 25(OH)D_3 levels and alkaline phosphatase activity across the experimental groups.

Characteristic/variable	Control	Vitamin D_3 deficiency	Vitamin D_3 administration
Total calcium, mM·L^{-1}	2.24±0.04	1.58±0.01*	2.1±0.02*, **
Protein-bound calcium, mM·L^{-1}	0.20±0.01	0.18±0.02	0.19±0.01**
Ultrafiltered calcium, mM·L^{-1}	2.04±0.01	1.40±0.01*	1.91±0.02*, **
Inorganic phosphate, mM·L^{-1}	2.1±0.01	1.46±0.02*	1.78±0.04*, **
Total activity of ALP, IU/L	230.2±2.7	386.0±4.0*	281.0±1.9*,**
Activity of intestinal ALP isoenzyme, IU/L	48.9±2.2	73.0±1.7*	61.9±0.4*,**
Activity of bone ALP isoenzyme, IU/L	190.9±4.3	320.2±3.9*	269.0±1.6*,**
25(OH)D_3, ng/mL (nmol/L)	47.30±7.20 (118.27±18.05)	7.78±0.60* (19.45±1.52*)	31.30±9.03** (78.24±22.57**)
PTH, pg/mL	256.0±20.5	448.1±38.0*	357.0±12.5*,**
FGF23, pg/mL	169.8±13.6	436.6±18.9*	169.0±11.2**

All data are presented as mean ± SD (n = 8 per group). The experimental groups included: 1) Intact group (maintained on a balanced diet for 3 months); 2) VD_3-deficient group (maintained on a VD_3-deficient diet for the entire 3-month period); 3) VD_3-supplemented group (received cholecalciferol, 1,000 IU/kg, for 1 month following a 2-month VD_3-depletion period). *$p < 0.05$ *vs.* the intact group; **$p < 0.05$ *vs.* the VD_3-deficient group. ALP, alkaline phosphatase; PTH, parathyroid hormone; FGF23, fibroblast growth factor 23; 25(OH)D_3, 25-hydroxyvitamin D_3 (calcifediol); VD_3, vitamin D_3 (cholecalciferol).

oesters and serves as a critical biomarker for bone remodeling. The observed rise in total ALP was driven primarily by an almost 1.7-fold increase in bone-specific isoform activity, signaling an intensification of pro-resorptive processes in the skeletal tissue. Low VD_3 intake also induced a 1.5-fold enhancement in intestinal isoenzyme activity, which coincided with a 1.44-fold decline in serum phosphate levels relative to the controls.

During the investigation, a classic correlation was observed between serum 25(OH)D_3 concentrations and calcium balance. Rearing the animals on a deficient diet resulted in a marked 1.42-fold decrease in serum calcium levels (Table I). This cation is typically maintained within a narrow homeostatic range and exists in two primary forms: a protein-bound, biologically inactive pool and an ultrafilterable, active fraction. The latter consists predominantly of ionized calcium (~85%) alongside various anionic complexes, such as citrate and phosphate[21]. The ratio between these components varies under different physiological and pathological conditions. In our study, VD_3 hypovitaminosis did not significantly alter the protein-bound calcium content. Instead, the reduction in the total mineral pool was entirely attributed to a 1.46-fold decline in the biologically active, ultrafilterable fraction compared with the intact group. Administration of cholecalciferol to the hypovitaminotic rodents almost completely normalized both the 25(OH)D_3 levels and the associated parameters of mineral homeostasis.

In the VD_3-deficient group, hypocalcemia occurred concurrently with the development of secondary hyperparathyroidism (SHPT), evidenced by a statistically significant, approximately 2-fold elevation in serum parathyroid hormone relative to the intact group (Table I). This hypersecretion represents a compensatory mechanism aimed at promoting mineral mobilization from the skeleton to support systemic calcium balance[5]. Our findings illustrate the progression of SHPT as a direct consequence of compromised intestinal absorption during vitamin D_3 deprivation. The chronic persistence of this condition is associated with a heightened risk of reduced bone mineral density, potentially leading to osteopenia and osteoporosis. Importantly, sustained PTH elevation is known to stimulate the secretion of FGF23, a master regulator of phosphate homeostasis[6]. In the deficient state, we observed a significant 2.57-fold increase in circulating levels of this phosphatonin relative to control values; however, therapeutic administration of cholecalciferol fully restored both factors to baseline concentrations (Table I).

Vitamin D_3-binding protein (VDBP) serves as the principal carrier for all vitamin D_3 metabolites. Beyond transport, this globulin facilitates fatty acid delivery and promotes actin scavenging[22]. Emerging evidence also highlights its role in immune modulation, particularly in macrophage activation and complement-mediated neutrophil recruitment during inflammation[23]. Consequently, fluctuations in VDBP concentrations may provide insights into vitamin D_3 status across various bio-

logical compartments, including the CNS. Despite its significance, the regulation of VDBP in specific organs under VD_3 deficiency remains poorly understood. Our analysis revealed that VD_3 depletion led to a significant elevation in VDBP protein levels: 1.20-fold in cerebral specimens (Figure 1A) and 1.36-fold in osseous tissue (Figure 2A) compared with their respective intact controls. Following cholecalciferol supplementation, VDBP expression remained elevated at both sites, with no significant reversal toward baseline levels observed in intact animals.

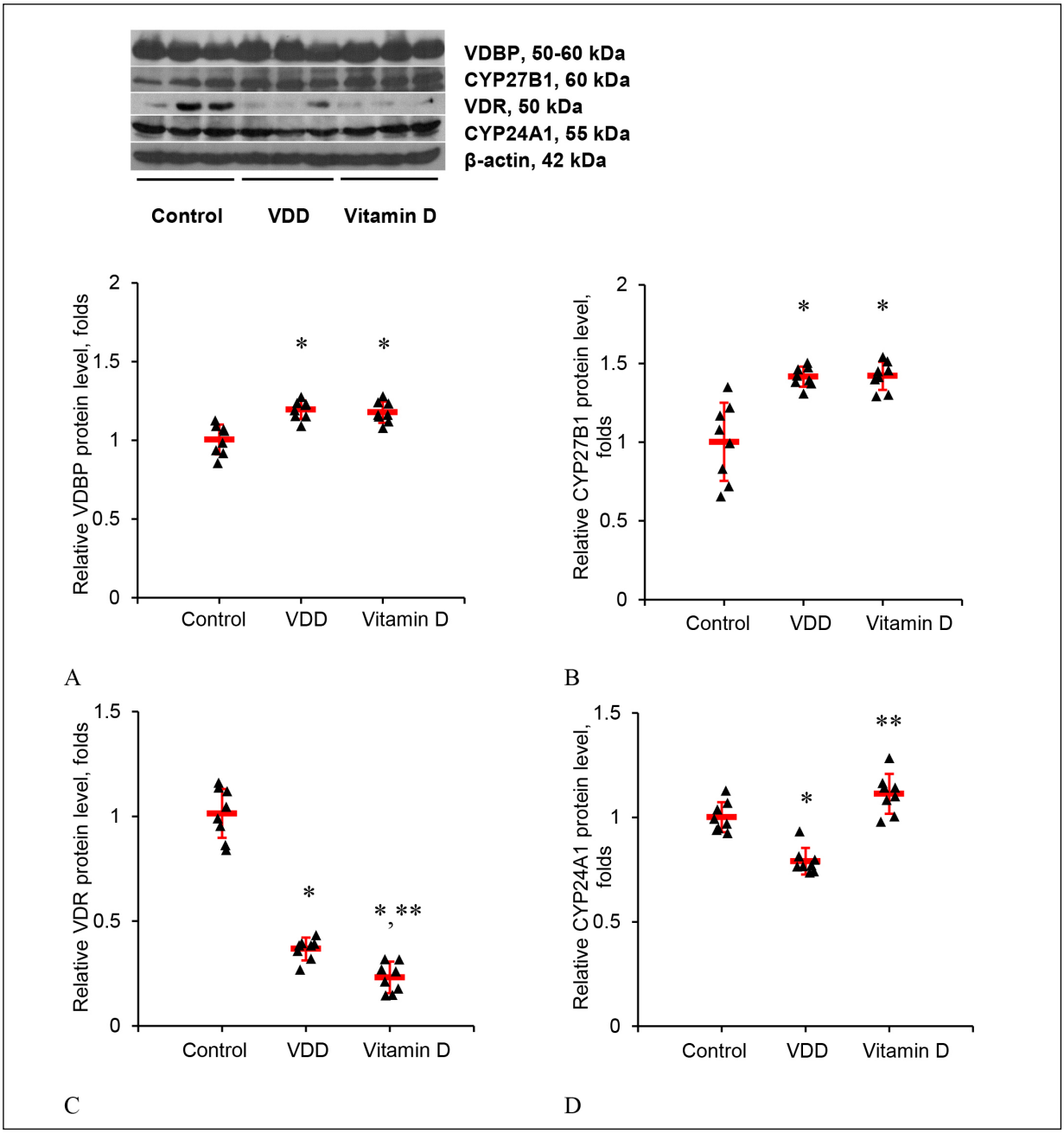

Figure 1. Relative protein expression of cerebral vitamin D_3 system components across the experimental groups. Panels represent: (**A**) VDBP; (**B**) CYP27B1; (**C**) VDR; (**D**) CYP24A1. Representative immunoblots are displayed above the corresponding scatter dot plots. To ensure analytical consistency, all target markers from the same experimental series were analyzed on parallel gels using a single master mix and quantified relative to a common internal β-actin control. Data are presented as individual data points with mean ± SD (n = 8 per group). The experimental groups included: 1) Intact group (maintained on a balanced diet for 3 months); 2) VD_3-deficient group (maintained on a VD_3-deficient diet for the entire 3-month period); 3) VD_3-supplemented group (received cholecalciferol, 1,000 IU/kg, for 1 month following a 2-month VD_3-depletion period). *$p < 0.05$ *vs.* the intact group; **$p < 0.05$ *vs.* the VD_3-deficient group. VDBP, vitamin D_3 binding protein; CYP27B1, 25-hydroxyvitamin D_3 1α-hydroxylase; VDR, vitamin D_3 receptor; CYP24A1, 25-hydroxyvitamin D_3-24-hydroxylase; VD_3, vitamin D_3 (cholecalciferol).

The classical pathway of VD_3 activation is driven by CYP27B1 (25-hydroxyvitamin 1α-hydroxylase). Traditionally localized in the renal proximal tubules, this enzyme converts $25(OH)D_3$ into its active hormonal form, $1\alpha,25(OH)_2D_3$[24]. It is now recognized that extrarenal expression of CYP27B1 enables local synthesis of the hormone, facilitating auto- and paracrine regulation of cellular functions (non-calcemic effects). In this study, VD_3 hypovitaminosis induced a marked increase in CYP27B1 protein content: 1.42-fold in the brain (Figure 1B) and 2.20-fold in the skeleton (Figure 2B) *vs.* the intact group. This upregulation likely represents a compensatory response to dimin-

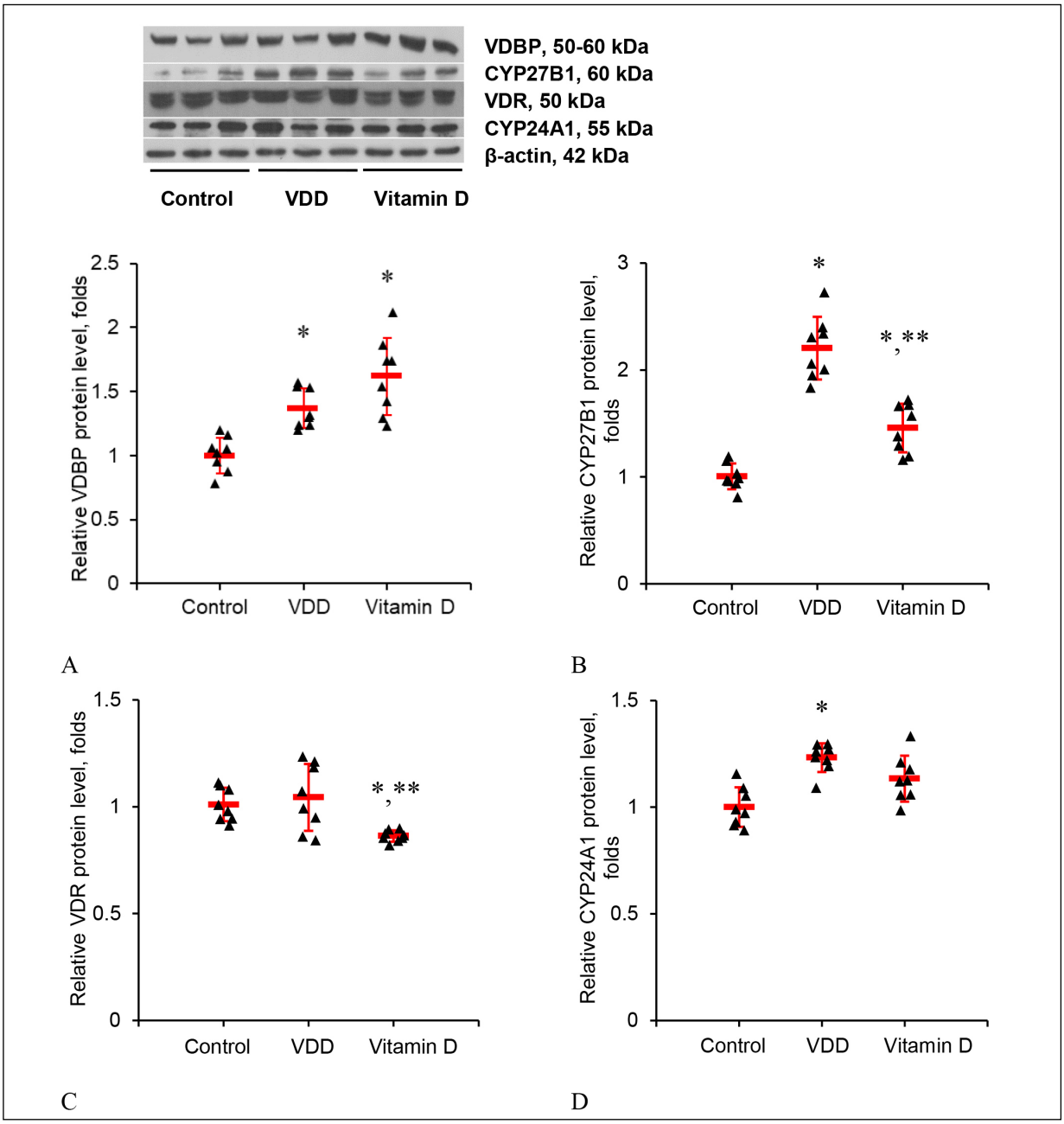

Figure 2. Relative protein expression of osseous vitamin D_3 system components across the experimental groups. Panels represent: (**A**) VDBP; (**B**) CYP27B1; (**C**) VDR; (**D**) CYP24A1. Representative immunoblots are displayed above the corresponding scatter dot plots. To ensure analytical consistency, all target markers from the same experimental series were analyzed on parallel gels using a single master mix and quantified relative to a common internal β-actin control. Data are presented as individual data points with mean ± SD (n = 8 per group). The experimental groups included: 1) Intact group (maintained on a balanced diet for 3 months); 2) VD_3-deficient group (maintained on a VD_3-deficient diet for the entire 3-month period); 3) VD_3-supplemented group (received cholecalciferol, 1,000 IU/kg, for 1 month following a 2-month VD_3-depletion period). *$p < 0.05$ *vs.* the intact group; **$p < 0.05$ *vs.* the VD_3-deficient group. VDBP, vitamin D_3 binding protein; CYP27B1, 25-hydroxyvitamin D_3 1α-hydroxylase; VDR, vitamin D_3 receptor; CYP24A1, 25-hydroxyvitamin D_3-24-hydroxylase; VD_3, vitamin D_3 (cholecalciferol).

ished substrate levels ($25(OH)D_3$) or disrupted VDR signaling. Notably, while VD_3 supplementation did not appreciably alter enzyme expression in neural tissue, it substantially reduced enzyme levels in osseous samples compared with the hypovitaminotic state.

Since the biological effects of calcitriol are mediated through its specific receptor (VDR), we investigated alterations in receptor expression across different vitamin D_3 statuses. Hypovitaminosis resulted in a significant 2.78-fold decrease in VDR protein within the cerebral compartment (Figure 1C), whereas its expression in bone remained stable (Figure 2C) relative to the intact group. Subsequent VD_3 administration resulted in a slight reduction in protein abundance, and cerebral VDR levels showed no recovery compared with the intact group.

The localized VD_3 auto-/paracrine system also involves CYP24A1 (24-hydroxylase), a mitochondrial monooxygenase found in most mammalian cells[25]. This regulatory enzyme mediates the inactivation of $1\alpha,25(OH)_2D_3$ and $25(OH)D_3$ through side-chain oxidation, converting them into metabolites with markedly diminished biological activity. In this capacity, CYP24A1 protects the organism from potential calcitriol toxicity[25]; thus, its regulation is a key mechanism by which target cells modulate their hormonal response. Deficient animals exhibited a 1.26-fold decline in cerebral CYP24A1 protein (Figure 1D). In contrast, enzyme expression in the osseous tissue increased 1.24-fold (Figure 2D). While VD_3 restoration did not significantly affect the catabolic enzyme content in the skeleton, it stimulated the synthesis of this cytochrome in the brain, effectively restoring it to baseline levels.

Given the intricate association between VD_3-metabolizing cytochromes, VDR expression, and FGF23, we finally sought to determine whether local FGF23 levels exhibit tissue-specific regulatory patterns distinct from the systemic profile. Consequently, we quantified the growth factor's content directly in both bone and brain specimens. A significant 1.76-fold increase in local FGF23 was observed in the skeletal matrix of the hypovitaminotic group compared with controls (Figure 3A). This increase was partially attenuated following cholecalciferol administration. In contrast, no significant shifts in FGF23 levels were detected in cerebral samples across all experimental groups (Figure 3B), highlighting a remarkably stable local profile despite systemic disturbances and high circulating phosphatonin levels.

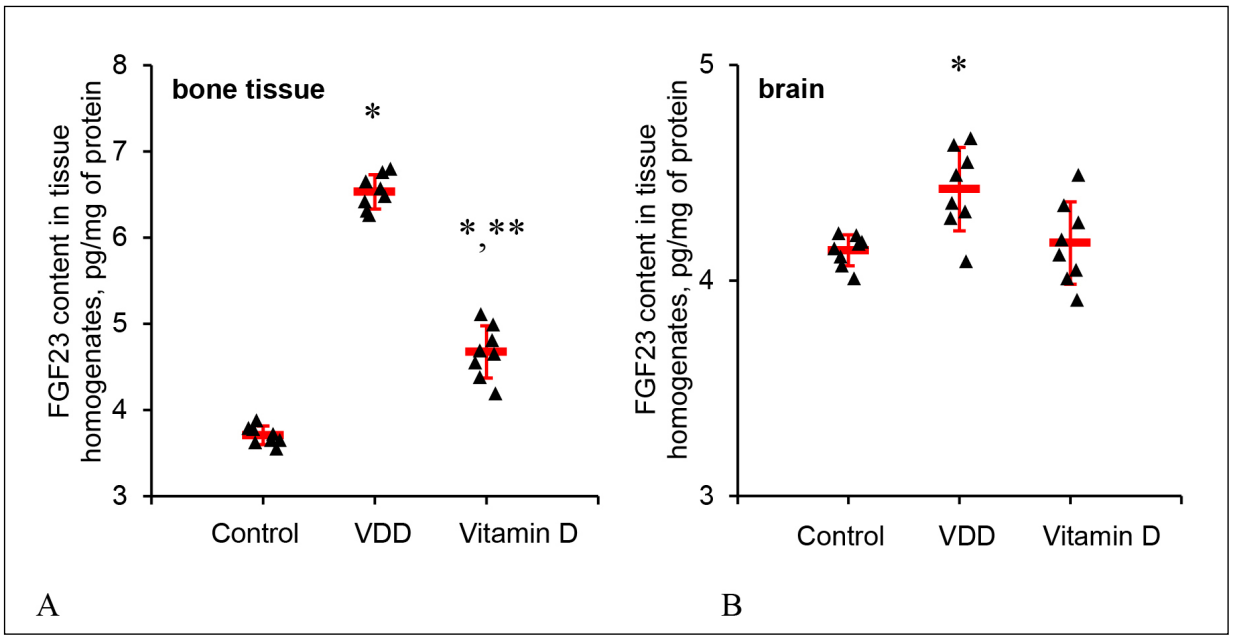

Figure 3. Local FGF23 levels in tissue homogenates across the experimental groups. Panels represent: (**A**) osseous tissue and (**B**) cerebral tissue. FGF23 concentrations were quantified *via* ELISA and normalized to total protein content as determined by the Lowry method. To address potential matrix effects, the assay was validated using linearity-of-dilution tests for each tissue type. Data are presented as scatter dot plots of individual data points with mean ± SD (n = 8 per group). The experimental groups included: 1) Intact group (maintained on a balanced diet for 3 months); 2) VD_3-deficient group (maintained on a VD_3-deficient diet for the entire 3-month period); 3) VD_3-supplemented group (received cholecalciferol, 1,000 IU/kg, for 1 month following a 2-month VD_3-depletion period). *$p < 0.05$ *vs.* the intact group; **$p < 0.05$ *vs.* the VD_3-deficient group. FGF23, fibroblast growth factor 23; VD_3, vitamin D_3 (cholecalciferol).

DISCUSSION

The present investigation explored the impact of systemic vitamin D_3 deficiency and subsequent short-term repletion on the local metabolic environment of both bone and brain tissues. By evaluating key regulatory components – VDR, VDBP, and the hydroxylases CYP27B1 and CYP24A1 – we aimed to delineate how different physiological compartments adapt to fluctuations in mineral homeostasis. Our findings reveal a complex landscape of adaptive responses, characterized by distinct tissue-specific expression patterns that suggest a divergence between systemic endocrine control in the skeleton and a more localized regulatory profile within the CNS.

A primary observation in our study was the concurrent upregulation of VDBP and CYP27B1 in both skeletal and cerebral specimens during VD_3 deprivation. The increase in VDBP expression likely represents a unified compensatory mechanism designed to enhance the sequestration and retention of available VD_3 metabolites within the tissue microenvironment[26]. By increasing the local pool of the carrier protein, the tissues may facilitate more efficient delivery of substrates to the activating enzymes. This is complemented by the induction of the 1α-hydroxylase CYP27B1, which suggests an autocrine attempt to maintain adequate levels of active $1\alpha,25(OH)_2D_3$ despite systemic depletion. Such localized upregulation of the activating machinery is well documented in extrarenal sites, where it preserves the non-canonical functions of vitamin D_3, including cell differentiation and immune modulation[27].

However, the regulation of the catabolic enzyme CYP24A1 and the hormone-receptor complex VDR marks a clear point of divergence between the two sites, potentially mediated by the osteoendocrine FGF23 system. In the skeleton, VD_3 depletion initiated a cascade of metabolic disturbances, including hypocalcemia and a compensatory rise in PTH, which, in turn, stimulated FGF23 secretion to regulate phosphate homeostasis[21,28]. Consequently, we observed a significant elevation of both serum and osseous FGF23 levels. According to classical feedback models, a state of low $1\alpha,25(OH)_2D_3$ should theoretically lead to the downregulation of the catabolic enzyme CYP24A1. However, our data show a paradoxical upregulation of CYP24A1 in bone tissue. It is plausible to hypothesize that within the osseous microenvironment, the stimulatory influence of elevated FGF23 predominates over the inhibitory signals of VD_3 deficiency. This sustained elevation of FGF23 and subsequent induction of CYP24A1 may exacerbate mineralization disorders, such as osteomalacia or osteoporosis, by limiting local VD_3 availability through accelerated degradation[29]. Notably, bone tissue retained a preserved VDR pool during the depletion phase, with protein levels remaining stable despite severe systemic hypovitaminosis.

In stark contrast, the CNS exhibited a marked reduction in both VDR and CYP24A1 levels during VD_3 deficiency. These results indicate a tissue-specific regulatory pattern that diverges from systemic endocrine loops. The suppression of the catabolic enzyme CYP24A1 in the brain is likely a protective adaptation aimed at minimizing the degradation of the active hormone, thereby preserving its concentration throughout the neural microenvironment[30,31]. Concurrently, the decrease in VDR expression may be attributed to a downregulation of receptor synthesis in response to the persistent deprivation of its primary ligand, $1\alpha,25(OH)_2D_3$. Unlike the skeleton, cerebral FGF23 levels remained remarkably stable throughout the study. This observation is consistent with reports suggesting that FGF23 acts predominantly as an endocrine hormone of osseous origin, targeting the renal-parathyroid axis rather than the CNS[32]. This lack of local FGF23 response in the brain, coupled with the downregulation of CYP24A1, underscores a discrete regulatory profile that may buffer neural tissue against systemic mineral fluctuations[30,33,34].

The subsequent cholecalciferol treatment further highlighted the differential sensitivity of these tissues. In the CNS, the rapid restoration of CYP24A1 levels suggests that the cerebral catabolic pathway is highly responsive to substrate availability, reflecting a capacity for localized control[34,35]. Conversely, cerebral VDR levels remained persistently reduced even after systemic VD_3 replenishment. This outcome may signify stable regulatory alterations, such as long-term epigenetic modifications – including DNA methylation or histone remodeling – of the *Vdr* promoter, induced by chronic hypovitaminosis[33,36,37]. While some research indicates that VDR expression remains relatively stable across the central nervous system irrespective of VD_3 status, our findings suggest a more dynamic or tissue-specific response to chronic deficiency[33].

In the skeletal compartment, the transition to vitamin D_3 sufficiency was marked by a pronounced downregulation of the activating enzyme CYP27B1. This rapid feedback inhibition occurred alongside a much more stable osseous VDR pool, which showed only a slight, though statistically significant, reduction in protein levels during the repletion period[38,39]. These observations imply that while the hydroxylase machinery is highly responsive to acute substrate fluctuations, the skeletal receptor apparatus maintains relative structural consistency during short-term recovery. Meanwhile, the refractory state of elevated matrix CYP24A1 points to the enduring influence of pathological remodeling and persistently high systemic FGF23 signals. Importantly, this lack of immediate normaliza-

tion extends to the local transport machinery; the continued elevation of VDBP in both cerebral specimens and the skeletal matrix reinforces the significance of the initial compensatory response. The fact that VDBP levels remained high despite treatment suggests a prolonged compensatory state or a slow turnover of the local VDBP pool, indicating that restoring substrate availability is insufficient to promptly reverse this upregulation.

Within this context, the stability of cerebral FGF23 alongside divergent hydroxylase expression represents a tissue-specific regulatory pattern rather than definitive proof of functional autonomy. While providing a basis for understanding the neuroskeletal axis, certain limitations must be considered. As our results are predicated on protein abundance, they may not strictly correlate with mRNA levels due to post-transcriptional mechanisms; thus, further verification *via* RT-qPCR is warranted. Additionally, Western blotting assesses bulk protein in lysates but does not delineate precise cellular co-localization or actual enzymatic activity – factors critical for VD_3-metabolizing hydroxylases. To ensure reliability across biological matrices, we used a multilevel normalization strategy, confirming that the observed fluctuations in VDR, VDBP, and CYP expression reflect consistent biological patterns rather than technical artifacts. Validation of the cerebral FGF23 profile further demonstrated that its homeostatic stability was independent of tissue-specific interference, highlighting a distinct regulatory environment in the brain compared to the endocrine-driven changes in osseous tissue.

By accounting for these methodological nuances, our findings provide reliable insights into tissue-specific expression patterns and serve as a descriptive foundation for further exploration. To build upon this framework, future studies should correlate protein profiles with precise cellular co-localization *via* immunohistochemistry. Additionally, functional assessments – such as evaluating neuronal viability, utilizing tracer-labeled VD_3, or conducting behavioral testing – are necessary to determine whether the observed profiles might represent a localized neuroprotective axis[40]. Ultimately, such multi-level validation is vital for delineating complex cellular interactions and elucidating the molecular drivers of the osteoendocrine bone-brain axis.

CONCLUSIONS

The results of this study demonstrate that vitamin D_3 deficiency elicits divergent, tissue-specific expression patterns in the brain and bone, reflecting distinct homeostatic profiles. Our data suggest that the brain may maintain a more stable internal FGF23 environment than bone, characterized by localized downregulation of the catabolic enzyme CYP24A1 and the absence of a marked response to systemic FGF23 fluctuations. In contrast, bone tissue exhibits notable susceptibility to systemic humoral factors; specifically, the FGF23 endocrine axis appears to play a major role, with elevated levels during deficiency potentially contributing to pathological bone remodeling and exacerbating mineral metabolic disorders. Furthermore, the persistent suppression of cerebral VDR expression following VD_3 supplementation suggests long-term regulatory shifts within the central nervous system that could differ from the more flexible feedback mechanisms observed in the skeleton. While these distinct findings are compatible with differential metabolic regulation, further functional studies are required to confirm the potential presence of a localized neuroprotective axis.

Conflict of Interest

The authors declare that the research was conducted in the absence of any commercial or financial relationships that could be construed as a potential conflict of interest.

Funding

This research was funded by the National Research Foundation of Ukraine (grant No. 2023.03/0222).

Authors' Contributions

Ihor Shymanskyi: conceptualization, methodology, investigation, data curation, original draft preparation.
Olha Lisakovska: methodology, validation, investigation, software, visualization.
Anna Khomenko: resources, validation, investigation.
Vasiliy Bilous: resources, investigation.
Yevhenii Kucheriavyi: resources, investigation.
Iryna Poladych: resources, investigation.
Yulya Parkhomenko: resources, investigation.
Mykola Veliky: supervision, funding acquisition, project administration, writing – review and editing. All authors have read and agreed to the published version of the manuscript.

Data Availability

The datasets generated during and/or analyzed during the current study are available from the corresponding author on reasonable request.

Ethics Approval

The experimental protocol was approved by the Animal Care Ethics Committee of the Palladin Institute of Biochemistry (Protocol #3, February 26, 2024).

ORCID ID

Ihor Shymanskyi: 0000-0002-1507-8906
Olha Lisakovska: 0000-0002-5844-1453
Anna Khomenko: 0000-0002-5523-6008
Vasiliy Bilous: 0000-0002-7411-6300
Yevhenii Kucheriavyi: 0000-0002-3269-0742
Iryna Poladych: 0000-0002-8494-2534
Yuliya Parkhomenko: 0000-0001-9102-0450
Mykola Veliky: 0000-0002-8125-308X

REFERENCES

1. Liu Y, Zhong Z, Xie J, Ni B, Wu Y. Neuroprotective roles of vitamin D: bridging the gap between mechanisms and clinical applications in cognitive decline. Int J Mol Sci 2025; 26: 7146.
2. Pál É, Ungvári Z, Benyó Z, Várbíró S. Role of vitamin D deficiency in the pathogenesis of cardiovascular and cerebrovascular diseases. Nutrients 2023; 15: 334.
3. Weller RB. Sunlight: Time for a rethink? J Invest Dermatol 2024; 144: 1724-1732.
4. Voltan G, Cannito M, Ferrarese M, Ceccato F, Camozzi V. Vitamin D: an overview of gene regulation, ranging from metabolism to genomic effects. Genes (Basel) 2023; 14: 1691.
5. Xiang Z, Wang M, Miao C, Jin D, Wang H. Mechanism of calcitriol regulating parathyroid cells in secondary hyperparathyroidism. Front Pharmacol 2022; 13: 1020858.
6. Martínez-Heredia L, Canelo-Moreno JM, García-Fontana B, Muñoz-Torres M. Non-classical effects of FGF23: molecular and clinical features. Int J Mol Sci 2024; 25: 4875.
7. Latic N, Erben RG. FGF23 and vitamin D metabolism. JBMR Plus 2021; 5: e10558.
8. Hansda S, Das H. Unraveling the bone-brain communication network. Biology (Basel) 2025; 14: 1279.
9. Liang TZ, Jin ZY, Lin YJ, Chen ZY, Li Y, Xu JK, Yang F, Qin L. Targeting the central and peripheral nervous system to regulate bone homeostasis: mechanisms and potential therapies. Mil Med Res 2025; 12: 13.
10. Liu M, Liu Y, Yu J, Gong J, Zhao C, Liu Z. Molecular mechanisms and therapeutic implications of the sympathetic nervous system in bone-related disorders: a brain-bone axis perspective. Bone Res 2025; 13: 98.
11. Shi T, Shen S, Shi Y, Wang Q, Zhang G, Lin J, Chen J, Bai F, Zhang L, Wang Y, Gong W, Shao X, Chen G, Yan W, Chen X, Ma Y, Zheng L, Qin J, Lu K, Liu N, Xu Y, Shi YS, Jiang Q, Guo B. Osteocyte-derived sclerostin impairs cognitive function during ageing and Alzheimer's disease progression. Nat Metab 2024; 6: 531-549.
12. Karasalih B, Duman H, Bechelany M, Karav S. Osteopontin: its properties, recent studies, and potential applications. Int J Mol Sci 2025; 26: 5868.
13. Li J, Lou S, Bian X. Osteocalcin and GPR158: linking bone and brain function. Front Cell Dev Biol 2025; 13: 1564751.
14. Ng JS, Chin KY. Potential mechanisms linking psychological stress to bone health. Int J Med Sci 2021; 18: 604-614.
15. Kim HK, Fukazawa A, Smith SA, Mizuno M, Rothermel BA, Fujikawa T, Galvan M, Gautron L, Pastor JV, Carroll IJ, Moe OW, Vongpatanasin W. High dietary phosphate intake induces hypertension and sympathetic overactivation via central fibroblast growth factor receptor signaling. Circulation 2025; 152: 450-464.
16. Amaravadi KSS, Nalisetty P, Vadlamani N, Ibrahimli S, Khan FA, Castillo JA, Penumetcha SS. Impact of elevated fibroblast growth factor 23 (FGF23) on the cardiovascular system: a comprehensive systematic literature review. Cureus 2024; 16: e59820.
17. Acquaviva J, Abdelhady HG, Razzaque MS. Phosphate dysregulation and neurocognitive sequelae. Adv Exp Med Biol 2022; 1362: 151-160.
18. Laszczyk AM, Nettles D, Pollock TA, Fox S, Garcia ML, Wang J, Quarles LD, King GD. FGF-23 deficiency impairs hippocampal-dependent cognitive function. eNeuro 2019; 6: ENEURO.0469-18.2019.
19. Bowers GN Jr, McComb RB. Measurement of total alkaline phosphatase activity in human serum. Clin Chem 1975; 21: 1988-1995.
20. Laemmli UK. Cleavage of structural proteins during the assembly of the head of bacteriophage T4. Nature 1970; 227: 680-685.
21. Matikainen N, Pekkarinen T, Ryhänen EM, Schalin-Jäntti C. Physiology of calcium homeostasis: an overview. Endocrinol Metab Clin North Am 2021; 50: 575-590.
22. Hazeldine J, Dinsdale RJ, Naumann DN, Acharjee A, Bishop JRB, Lord JM, Harrison P. Traumatic injury is associated with reduced deoxyribonuclease activity and dysregulation of the actin scavenging system. Burns Trauma 2021; 9: tkab001.
23. Delanghe JR, Delrue C, Speeckaert R, Speeckaert MM. The potential role of vitamin D binding protein in kidney disease: a comprehensive review. Acta Clin Belg 2024; 79: 130-142.
24. Oczkowicz M, Szymczyk B, Świątkiewicz M, Furgał-Dzierżuk I, Koseniuk A, Wierzbicka A, Steg A. Analysis of the effect of vitamin D supplementation and sex on Vdr, Cyp2r1 and Cyp27b1 gene expression in Wistar rats' tissues. J Steroid Biochem Mol Biol 2021; 212: 105918.
25. Milan KL, Ramkumar KM. Regulatory mechanisms and pathological implications of CYP24A1 in vitamin D metabolism. Pathol Res Pract 2024; 264: 155684.
26. Kresge HA, Blostein F, Goleva S, Albiñana C, Revez JA, Wray NR, Vilhjálmsson BJ, Zhu Z, McGrath JJ, Davis LK. Phenomewide association study of health outcomes associated with the genetic correlates of 25 hydroxyvitamin D concentration and vitamin D binding protein concentration. Twin Res Hum Genet 2024; 27: 69-79.
27. Bikle DD, Patzek S, Wang Y. Physiologic and pathophysiologic roles of extra renal CYP27b1: case report and review. Bone Rep 2018; 8: 255-267.
28. Latic N, Erben RG. Interaction of vitamin D with peptide hormones with emphasis on parathyroid hormone, FGF23, and the Renin-Angiotensin-Aldosterone system. Nutrients 2022; 14: 5186.
29. Verlinden L, Carmeliet G. Integrated view on the role of vitamin D actions on bone and growth plate homeostasis. JBMR Plus 2021; 5: e10577.
30. Bikle DD. Vitamin D: Newer concepts of its metabolism and function at the basic and clinical level. J Endocr Soc 2020; 4: bvz038.
31. Gezen-Ak D, Dursun E, Yilmazer S. Vitamin D inquiry in hippocampal neurons: consequences of vitamin D-VDR pathway disruption on calcium channel and the vitamin D requirement. Neurol Sci 2013; 34: 1453-1458.
32. Ursem SR, Diepenbroek C, Bacic V, Unmehopa UA, Eggels L, Maya-Monteiro CM, Heijboer AC, la Fleur SE. Localization of fibroblast growth factor 23 protein in the rat hypothalamus. Eur J Neurosci 2021; 54: 5261-5271.
33. Liu H, He Y, Beck J, da Silva Teixeira S, Harrison K, Xu Y, Sisley S. Defining vitamin D receptor expression in the brain using a novel VDRCre mouse. J Comp Neurol 2021; 529: 2362-2375.
34. Cui X, Eyles DW. Vitamin D and the Central Nervous System: causative and preventative mechanisms in brain disorders. Nutrients 2022; 14: 4353.
35. Landel V, Stephan D, Cui X, Eyles D, Feron F. Differential expression of vitamin D-associated enzymes and receptors in brain cell subtypes. J Steroid Biochem Mol Biol 2018; 177: 129-134.
36. Gasperini B, Falvino A, Piccirilli E, Tarantino U, Botta A, Visconti VV. Methylation of the vitamin D receptor gene in human disorders. Int J Mol Sci 2023; 25: 107.

37. Fetahu IS, Höbaus J, Kállay E. Vitamin D and the epigenome. Front Physiol 2014; 5: 164.
38. Adams JS, Rafison B, Witzel S, Reyes RE, Shieh A, Chun R, Zavala K, Hewison M, Liu PT. Regulation of the extrarenal CYP27B1-hydroxylase. J Steroid Biochem Mol Biol 2014; 144 Pt A: 22-27.
39. St-Arnaud R, Dardenne O, Prud'homme J, Hacking SA, Glorieux FH. Conventional and tissue-specific inactivation of the 25-hydroxyvitamin D-1alpha-hydroxylase (CYP27B1). J Cell Biochem 2003; 88: 245-251.
40. Fraser DR. Perspective: vitamin D deficiency relationship to initiation of diseases. Nutrients 2025; 17: 2900.